Journal of Solid State Chemistry 181 (2008) 2191–2198

Contents lists available at ScienceDirect

Journal of Solid State Chemistry

journal homepage: www.elsevier.com/locate/jssc

The role of intermolecular interactions in the assemblies of Fe^{II} and Co^{II} tetrakis-isothiocyanatometalates with tris(1,10-phenanthroline)-Ru^{II}: Crystal structures of two dual-metal assemblies featuring octahedral cationic and tetrahedral anionic modules

Mohamed Ghazzali *, Vratislav Langer, Lars Öhrström

Department of Chemical and Biological Engineering, Chalmers University of Technology, SE-412 96 Göteborg, Sweden

ARTICLE INFO

Article history:
Received 29 January 2008
Received in revised form
16 April 2008
Accepted 27 April 2008
Available online 10 May 2008

Keywords:
Dual-metals
Racemates
Double-helices
X-ray single-crystal structure determination
Hydrogen bonding
S···S intermolecular interaction

ABSTRACT

Two new dual-metal assemblies: $2[Ru(phen)_3]^{2+}\cdot[Fe(SCN)_4]^{2-}\cdot 2SCN^-\cdot 4H_2O$ **1** and $[Ru(phen)_3]^{2+}\cdot[Co(SCN)_4]^{2-}$ **2**, (phen:1,10-phenanthroline), have been prepared and their structures were characterized by X-ray diffraction. In **1**, the cationic octahedral enantiomers are arranged with a $\Lambda\Lambda\Lambda\Lambda\Lambda\Lambda$ sequence supported by π–π stacking and the anionic inorganic tetrahedral units are oriented between these stacks by interacting with the nearby water molecules through strong O–H···O and O–H···S hydrogen bonds. In **2**, homochiral double helices in the *b*-direction are revealed, with tetrakis-isothiocyanate Co^{II} anions arranged in the crystal to furnish one-dimensional (1D)-helical chains with S···S intermolecular interactions at 3.512(2) and 3.966(2) Å supporting $[Ru(phen)_3]^{2+}$ Λ- and Δ-helices with Ru···Ru shortest distance of 8.676(7) Å. In both **1** and **2**, the supramolecular assembly is maintained by C–H···S hydrogen bonds extending between the phenanthroline aromatic carbons in the cationic nodes and the sulphur atoms of the isothiocyanates anions. Analysis of S···S interactions in isothiocyanate containing compounds using Cambridge structural database (CSD) showed an angle dependence categorizing these interactions into "type-I" and "type-II".

1. Introduction

An effective way to get benefit of the features existing in both coordination and inorganic complexes is to mix them in one material. Mixed metal assemblies that possess both coordination and inorganic complexes as cationic and anionic nodes are of a growing interest in the crystal engineering of supramolecular architectures [1]. Such assemblies can exhibit many functional properties like imitating the redox behaviour of the diffused metal ions in the solid state as well as being candidates for molecule-based magnetic materials and non-linear optical materials [2,3]. Specifically, the intermolecular interactions, e.g. hydrogen bonds, π–π stacking and dipole–dipole interactions, provided by these systems, can determine the route for charge exchange between the ionic centres [4]. In most of these materials, supramolecular architecture is maintained due to the long-range interactions between the inorganic centres that are separated by coordination complexes resulting in a structure comprising a framework separated by weakly interacting organic domains [5,6].

Fritsky et al. [5] have shown examples of cation–anion assemblies and emphasized the different intermolecular interactions in [Ni(1,10-phenanthroline)$_3$][Cu[bis(hydroxyiminopropionyl)-1,3 diaminopropane)]$_2$(NO_3)$\cdot 8H_2O$ [7]. Recently, Feng et al. [8] employed $[Ru(1,10\text{-phenanthroline})_3]^{2+}$ cations as templates to organize Cd^{II} inorganic clusters into either molecular crystals or three-dimensional (3D) covalent open frameworks, while Dong et al. [9] used an anionic cluster made from $I^-\cdot(H_2O)_6$ and $[Fe(CN)_6\cdot H_2O]^{2-}$ as a 3D host for [Ru-(bi-pyridinyl)$_3$]$^{2+}$ cations.

Here, we have employed the octahedral propeller-like complex tris(1,10-phenanthroline) ruthenium(II), $[Ru(phen)_3]^{2+}$, used in many studies of redox potentials, excited-state reactivity, photochemistry and energy transfer as well as probing and dying of DNA cleavages [10], as the coordination complex module. Transition metal tetra-isothiocyanate complexes $[M(SCN)_4]^{2-}$ are also well-implemented in crystal engineering [3,11], and are used here as the anionic building blocks. SCN^- is an ambidentate low-field ligand with hard N atoms and softer S atoms hence ensuring a degree of polarizability that eventually can lead to extended polymeric structures of metal complexes [12].

We here present syntheses and crystal structures of two such dual-metal assemblies where M is Fe^{2+} in **1**, with the formula $\{2[RuC_{36}N_6H_{24}]^{2+}\cdot[Fe(NCS)_4]^{2-}\cdot 2(NCS)^-\ 4H_2O\}$ and Co^{2+} in **2**,

* Corresponding author. Fax: +46 31 772 3858.
E-mail address: mghazz@chalmers.se (M. Ghazzali).

0022-4596/$ - see front matter © 2008 Elsevier Inc. All rights reserved.
doi:10.1016/j.jssc.2008.04.039

with the formula $\{[RuC_{36}N_6H_{24}]^{2+}.[Co(NCS)_4]^{2-}\}$. In addition, we are extending our interest in the intermolecular interactions caused by halogens, e.g. Br···Br interactions [13] with those caused by chalcogens, particularly S···S interactions by an analysis of isothiocyanates containing fragments in Cambridge structural database (CSD), complemented with a quantum chemistry model study.

2. Experimental

2.1. Synthesis of the title compounds

All chemicals were obtained from the Aldrich Chemical Co. and used without further purification. IR spectra were recorded on Perkin-Elmer instrument with resolution of $4\,cm^{-1}$. **1** was prepared as follows: A solution of iron(II) perchlorate hexahydrate [0.2 mmol, 0.06 g] and potassium thiocyanate [0.4 mmol, 0.04 g] in 15 mL MeOH/EtOH/MeCN [1:1:1] was stirred for 30 m at room temperature under N_2 stream followed by filtration. To the filtrate, a 20 mL MeOH/EtOH (1:1) solution of tris-(1,10 phenanthroline)-ruthenium (II) chloride (0.1 mmol, 0.08 g) was poured carefully. The resulting solution was set aside and crystallized at room temperature. Dark red plates with low yield (<10%) were collected after 1 week and dried in air.

Caution: Perchlorate salts of metal complexes are potentially explosive. Only small quantities of the compound should be prepared and handled with care!

IR(γ,1/cm,KBr):618(m)[π_{CH}],840(m)[δ_{CH}],1122(s)[$C=S$],1410(m)[$OH_{bending}$],1635(m)[$C=C$], 2060(s)[$-N^{+}\equiv C^{-}$],3430(s)[OH].

2 was prepared as follows: A solution of cobalt(II) chloride hexahydrate [0.2 mmol, 0.05 g] and potassium thiocyanate [0.4 mmol, 0.04 g] in 15 mL MeOH/EtOH/MeCN [1:1:1] was stirred for 30 m at room temperature under N_2 stream followed by filtration. To this filtrate, a 10 mL MeOH/EtOH (1:1) solution of tris-(1,10 phenanthroline)-ruthenium (II) chloride (0.1 mmol, 0.08 gm) was allowed to diffuse slowly. The resulting solution was set aside. Red plates with low yield (<10%) were grown at room temperature and collected after 1 week and dried in air.

IR(γ,1/cm,KBr):622(m)[π_{CH}],723(m)[$CH_{bending}$],843(m)[δ_{CH}],1080(s)[$C=S$],1570(m) [$C=C$], 2050(s) [$-N^{+}\equiv C^{-}$],3080(s)[= C–H].

Table 1
Crystal data and refinement parameters for structures **1** and **2**

Empirical formula	$C_{78}H_{56}FeN_{18}O_4Ru_2S_6$	$C_{40}H_{24}CoN_{10}RuS_4$
Molecular formula	$2(RuC_{36}N_6H_{24})^{2+}\cdot Fe(SCN)_4^{2-}\cdot 2(SCN)^{-}\cdot 4H_2O$	$(RuC_{36}N_6H_{24})^{2+}\cdot Co(SCN)_4^{2-}$
Molecular weight	1759.76	932.93
space group	$C2/c$	$P2_1/n$
Z	4	8
D_{calc} ($g\,cm^{-3}$)	1.561	1.605
a (Å)	18.799 (3)	12.9217 (7)
b (Å)	16.453 (2)	16.3453 (9)
c (Å)	24.510 (4)	36.656 (2)
β (deg)	98.933 (3)	94.024 (1)
Unit cell volume (Å^3)	7489.1 (19)	7723.0 (7)
Crystal dimension (mm)	$0.24\times0.05\times0.03$	$0.63\times0.21\times0.11$
Reflections collected	30,645 measured reflections	93,174 measured reflections
	6673 independent reflections	15,833 independent reflections
	3688 reflections with $I>2\sigma(I)$	11,114 reflections with $I>2\sigma(I)$
θ range (deg)	2.2–25.2	2.0–26.4
R_{int} [$2\sigma_I$]	0.131	0.080
R-indices [$I>2\sigma_I$]	$R_1=0.059$, $wR_2=0.132$	$R_1=0.047$, $wR_2=0.101$
Goodness-of-fit	1.02	1.03
Data/parameters/restraints	6673/504/6	15833/1009/0
Highest peak/deepest hole	0.86/–1.00	1.08/–1.01
Common parameters: scan method: ω-scan, Temp.: 153 K, $\lambda=0.71073$ Å, crystal system: monoclinic		

2.2. X-ray single-crystal diffraction

Suitable single crystals of the title compounds (**1** and **2**) were selected and mounted onto tips of thin glass capillaries. Diffraction data were collected using a Siemens SMART CCD diffractometer with Mo$K\alpha$ radiation ($\lambda=0.71073$ Å, graphite monochromator). The crystals were cooled to 153(2) K by a flow of nitrogen gas using the LT-2A device. Full spheres of reciprocal spaces were scanned by 0.3° steps in ω with a crystal-to-detector distance of 3.97 cm. Preliminary orientation matrices were obtained from the first frames using SMART [14]. The collected frames were integrated using the preliminary orientation matrices which were updated every 100 frames. Final cell parameters were obtained by refinement of the positions of reflections with $I>10\sigma_I$

Table 2
Selected bond distances (Å) and angles (deg) for structures **1** and **2**

Ru1–1	2.052(6)	N2–Ru1–N4	98.1(2)
Ru1–N2	2.056(5)	N2–Ru1–N5	172.2(2)
Ru1–N3	2.061(5)	N3–Ru1–N5	94.2(2)
Ru1–N4	2.072(5)	N3–Ru1–N6	172.4(2)
Ru1–N5	2.062(6)	N1–Ru1–N4	175.9(2)
Ru1–N6	2.063(6)	N5–Ru1–N4	88.8(2)
Fe2–N7^{i}	2.023(8)	N5–Ru1–N6	80.0(2)
Fe2–N7	2.023(8)	N2–Ru1–N6	95.7(2)
Fe2–N8	2.042(7)	N6–Ru1–N4	95.2(2)
Fe2–N8^{i}	2.042(7)	N1–Ru1–N6	88.7(2)
		N7–Fe2–N7^{i}	114.7(5)
N1–Ru1–N2	80.4(2)	N7–Fe2–N8	112.7(3)
N1–Ru1–N3	96.7(2)	N7^{i}–Fe2–N8	101.9(3)
N2–Ru1–N3	90.6(2)	N7–Fe2–N8^{i}	101.9(3)
N3–Ru1–N4	79.5(2)	N7^{i}–Fe2–N8	112.7(3)
N1–Ru1–N5	92.9(2)	N8–Fe2–N8^{i}	113.4(4)
Symmetry code:(i) $-x$, y, $-z+1/2$			
Ru1A–N1A	2.065(3)	N1A–Ru1A–N2A	79.88(13)
Ru1A–N2A	2.073(3)	N5A–Ru1A–N1A	92.44(13)
Ru1A–N3A	2.068(3)	N5A–Ru1A–N6A	80.00(13)
Ru1A–N4A	2.069(3)	N1A–Ru1A–N6A	96.38(14)
Ru1A–N5A	2.045(3)	N8A–Co1A–N7A	111.0(2)
Ru1A–N6A	2.070(3)	N8A–Co1A–N9A	107.9(2)
Co1A–N7A	1.959(5)	N8A–Co1A–N10A	107.94(1)
Co1A–N8A	1.952(5)	N7A–Co1A–N9A	116.7(2)
Co1A–N9A	1.973(5)	N7A–Co1A–N10A	105.32(19)
Co1A–N10A	1.987(5)	N9A–Co1A–N10A	107.68(18)
Ru2B–N1B	2.058(3)	N1B–Ru2B–N4B	91.20(13)
Ru2B–N2B	2.070(3)	N4B–Ru2B–N3B	79.60(13)
Ru2B–N3B	2.072(3)	N1B–Ru2B–N2B	79.90(13)
Ru2B–N4B	2.062(3)	N1B–Ru2B–N3B	92.76(13)
Ru2B–N5B	2.071(3)	N1B–Ru2B–N5B	93.29(13)
Ru2B–N6B	2.074(3)	N6B–Ru2B–N5B	79.74(13)
Co2B–N7B	1.989(5)	N1B–Ru2B–N6B	171.83(13)
Co2B–N8B	1.962(5)	N4B–Ru2B–N6B	95.94(13)
Co2B–N9B	1.964(4)	N6B–Ru2B–N3B	92.42(13)
Co2B–N10B	1.950(5)	N4B–Ru2B–N2B	94.25(13)
N5A–Ru1A–N3A	93.51(13)	N6B–Ru2B–N2B	95.58(13)
N3A–Ru1A–N1A	172.12(13)	N3B–Ru2B–N2B	170.39(13)
N3A–Ru1A–N6A	89.74(13)	N4B–Ru2B–N5B	175.01(13)
N1A–Ru1A–N4A	94.25(13)	N3B–Ru2B–N5B	97.99(13)
N6A–Ru1A–N4A	97.10(13)	N2B–Ru2B–N5B	88.68(13)
N5A–Ru1A–N2A	92.86(13)	N9B–Co2B–N8B	111.41(18)
N6A–Ru1A–N2A	171.84(13)	N9B–Co2B–N10B	106.04(19)
N4A–Ru1A–N2A	90.44(13)	N8B–Co2B–N7B	111.96(19)
N5A–Ru1A–N4A	172.97(13)	N9B–Co2B–N7B	107.40(19)
N2A–Ru1A–N3A	94.66(13)	N10B–Co2B–N7B	113.58(19)
N3A–Ru1A–N4A	80.03(13)	N10B–Co2B–N8B	106.3(2)

after integration of all the frames using SAINT software. [14] The data were empirically corrected for absorption and other effects using the SADABS programme [15]. The structures were solved by direct methods and refined by full-matrix least squares on all $|F^2|$ data using SHELXTL software [16]. Hydrogen atoms of 1,10-phenanthroline ligands were constrained to ideal geometry with isotropic atomic displacement factor U_{iso}(H)1.2 times U_{eq} of the pivot atom and all non-hydrogen atoms were anisotropically refined. Figures were created using the DIAMOND package [17].

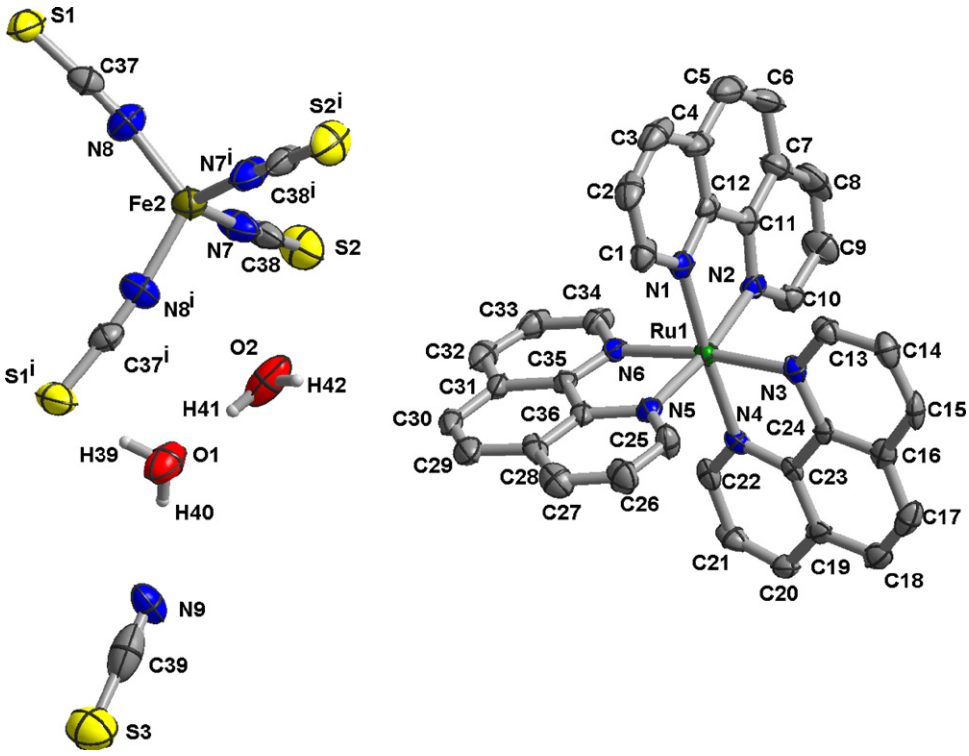

Fig. 1. Atomic numbering scheme of **1** with atomic displacement ellipsoids shown at 50% probability level. Hydrogen atoms of $[Ru(phen)_3]^{2+}$ were omitted for clarity. Symmetry code: (i)−*x*, *y*, −*z*+1/2.

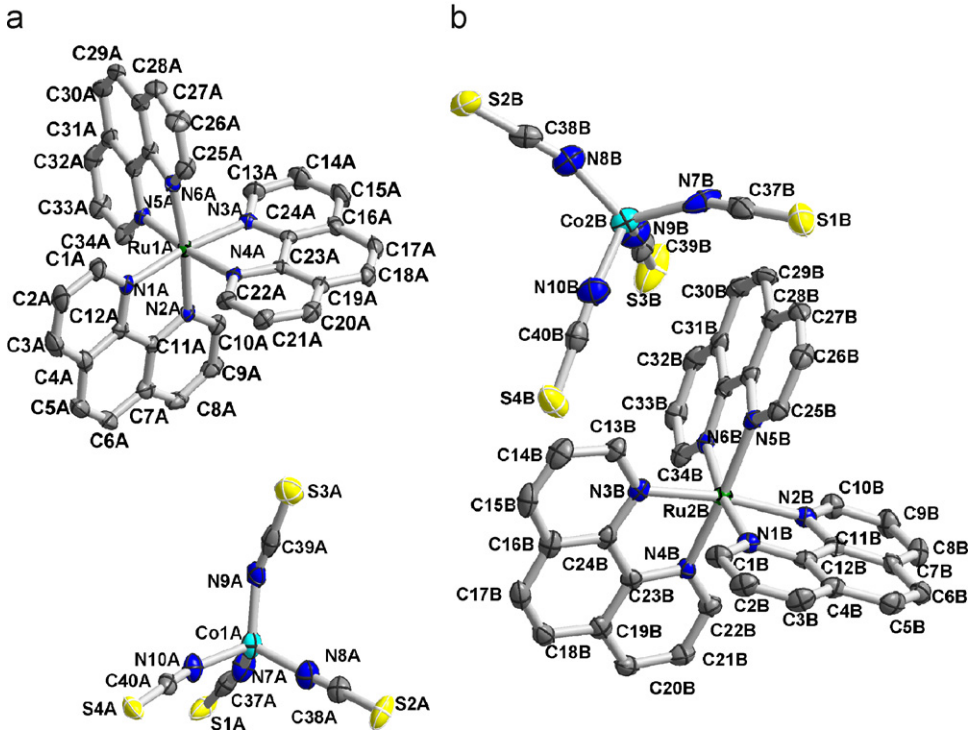

Fig. 2. (a, b) Labelling scheme of **2** with atomic displacement ellipsoids shown at 50% probability level. Hydrogen atoms were omitted for clarity.

2.3. Search in the CSD

Cambridge Structural Database, CSD, version 5.29, November 2007 [18] was screened. Sulphur and carbon atoms of the thiocyanate fragment were defined as bonded to one and two atoms, respectively. The non-bonded distance was constrainted to a range between 3.1 and 4.0 Å. The upper limit is $2r_{vdW}$ (3.6 Å) with a tolerance of 0.4 Å as interaction may occur up to this value [19], although it is slightly shorter than the revised $2r_{vdW}$ (4.06 Å) for sulphur bonded to carbon atom [20]. Error and disorder-free organometallic and organic structures with *R*-values lower than 10% were retrieved and analysed.

2.4. Computational details

Calculations were made with the DFT module in Spartan '06 [21] and start guess for $\{Zn(NCS)_2(NCSH)_2\}$ and SCNH fragments were carried out at the B3LYP/6-31+G* single point calculation and geometry was further optimized at the B3LYP/6-311+G** level of theory. The closed shell Zn^{2+} d^{10} ion was used instead of Co^{2+} and Fe^{2+} in order to simplify the calculation.

3. Results and discussions

The crystallographic data are given in Table 1, while selected bond distances and bond angles are given in Table 2. The thermal ellipsoid drawings for **1** and **2** with the atomic numbering schemes are shown in Figs. 1 and 2a and b, respectively. According to Dalhus and Görbitz [22], crystallization of racemates in *C*2/*c*, as in **1**, is of a low abundance (7.6%) while it is of the highest occurrence (57.1%) in $P2_1/c$. The overall geometry of the Ru^{II} complexes in **1** and **2** is pseudo octahedral. The Fe^{II} in **1** and the Co^{II} in **2** are exhibiting slightly distorted tetrahedral geometries.

In **1**, the Fe^{II} metal centres are situated on 2-fold rotational axes parallel to the *b*-crystallographic axis. In **2**, the asymmetric unit comprises two crystallographically independent $Co(SCN)_4^{2-}$ anions with two $[Ru(phen)_3]^{2+}$, shown in Fig. 2 as Λ-enantiomers.

The minimum inter-planar angle between the three phenanthroline ligands best-fit planes is 84.62 (8)° in **1**, while it is 79.90 (5)° in **2**. The minimum bite-angle of the phenanthroline ligands is 79.5 (2)° in **1** and 79.61 (13)° over the six bidentate ligands in **2,** which agrees with the previous published values for $[Ru(phen)_3]^{2+}$ complexes (79.8(2)° in [23a] and 80.0 (7)° in [23b]). The maximum deviation of the 6-membered ring from best-fit plane defined by the 1,10-phenanthroline ligands is 4.17 (1)° in **1**, while it is 2.92 (2)° in **2.**

The average Ru–N bond distance is 2.062(7) Å in **1** and 2.065(9) Å in **2**. The Fe–N average bond distance in **1** is 2.032(9) Å and the Co–N average bond distance in **2** is 1.967(13) Å, both ranges agree with values reported recently for Fe^{II} tetra-isothiocyanates [24] as well as those for Co^{II} tetra-isothiocyanates [25]. The maximum deviation from linearity in SCN^- groups is 3.46(3)° in **1** and 2.93(4)° in **2**.

The packing pattern of **1** in projection into *ac*-plane is shown in Fig. 3 while a projection into the *bc*-plane of **2** is given in Fig. 4. In both structures, the rigidity of the 1,10 phenanthroline ligands in $[Ru(phen)_3]^{2+}$ is a major key factor in the packing. The $[M(phen)_3]^{2+}$ complexes have three free pockets between the ligands, allowing intercalation of neighbouring molecules [23a,b,26]. In Fig. 3, we show how the stacked $\Lambda\Lambda$ $[Ru(phen)_3]^{2+}$ chains of enantiomer pairs in **1** are propagated along the *c*-axis and interloped by the $Fe(SCN)_4^{2-}$ anions. Enantiomer pairs in **1** (Fig. 5) are supported by a π–π stacking with an interplanar distance of 3.52(4) Å and C–H$\cdots\pi$ interactions at average distance of 2.88 Å, as calculated by PLATON [27] analysis for centroid$\cdots$centroid rings interaction. The shortest Ru$\cdots$Fe distance in **1** is 6.453(1) Å and the shortest Ru$\cdots$Co distance in **2** is 5.831(8) Å.

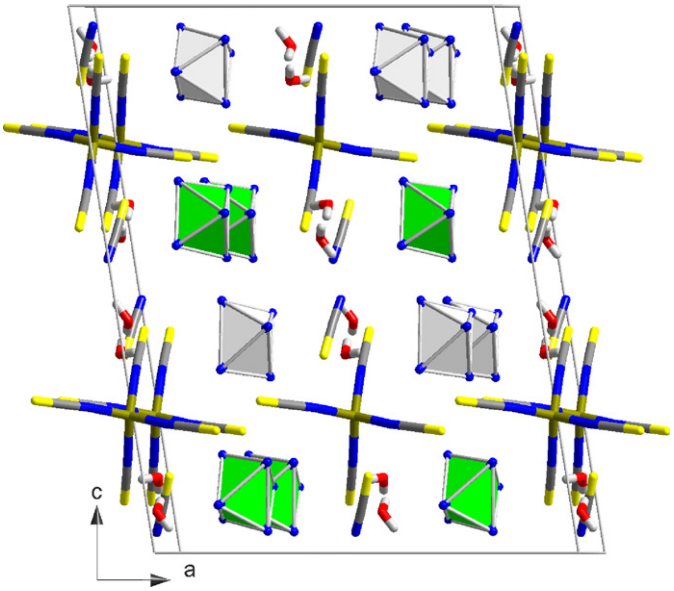

Fig. 3. Perspective drawing of **1** showing the packing pattern in projection along the *b*-axis. Λ- and Δ-$[Ru(phen)_3]^{2+}$ cations are represented as closed and open faces polyhedra, respectively.

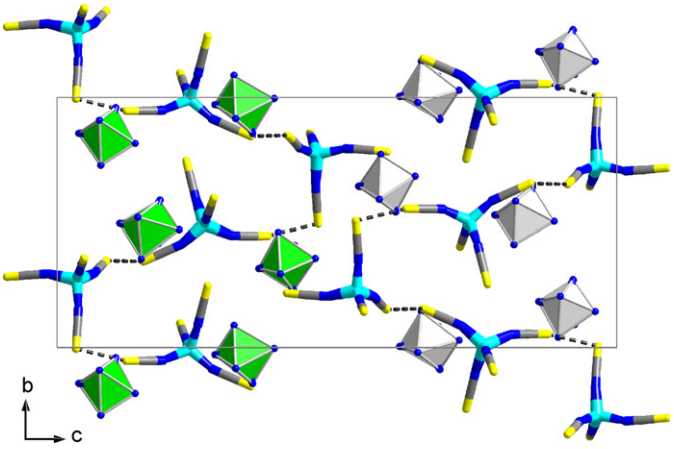

Fig. 4. Projection of **2** into *bc*-plane showing the packing pattern. Λ- and Δ-Ru(II)-tris(1,10-phenanthroline) cations are presented as closed and open faces polyhedra, respectively. S$\cdots$S intermolecular interactions are shown as dotted lines.

In **1,** the shortest Fe$\cdots$Fe distance is 12.49(3) Å and between the chains of $[Ru(phen)_3]^{2+}$, two water molecules and one free SCN^- counter ion are situated close to the $Fe[(SCN)_4]^{2-}$ anions. Such hydrophobic behaviour of $[Ru(phen)_3]^{2+}$ is probably a main cause for the complex binding ability when it comes in contact with the DNA grooves [28].

The $Fe[(SCN)_4]^{2-}$ anions, water solvates as well as the free SCN^- are interacting, in-between the cationic stacked molecules, through number of strong hydrogen bonds of O–H$\cdots$O, O–H$\cdots$S and O–H$\cdots$N types (Fig. 6). Geometrical parameters for hydrogen bonds in **1** and **2** are summarized in Table 3.

The $Fe[(SCN)_4]^{2-}$ anions are interconnected with the parallel stacks of $[Ru(phen)_3]^{2+}$ cations via weaker C–H$\cdots$S hydrogen bonds at D$\cdots$A average distance value of 3.74(4) Å.

Λ- and Δ-one-dimensional (1D)-helices of $[Ru(phen)_3]^{2+}$ cations are arranged in **2**, with a helix pitch of 16.345(1) Å, parallel with the *b*-axis, at minimum and maximum $[Ru(phen)_3]^{2+}$ helical separation distances of 11.094(6) and 14.838(7) Å (Fig. 7a). The $Co(SCN)_4^{2-}$ anions are arranged, in accordance with an S···S intermolecular interactions, into another 1D-helical chain (Fig. 7b). These homochiral double helices are extending to yield two helical packings being directed along the *b*-axis. Yet, no clear mechanism or cause for stimulating the homochiral packing in crystals is known [29]. $[Ru(phen)_3]^{2+}$ enantiomers in **2** are supported by C—H···π interaction at average H···π distance of 2.82 Å as well as by π–π stacking with a distance of 3.73(3) Å. $[Ru(phen)_3]^{2+}$ enantiomeric pairs are arranged in **1**, into 1D-zigzag pattern with a ΛΔΛΔΛ sequence (Fig. 5). The shortest Ru···Ru distance in **1** and **2** is 9.657(2) Å and 8.676(7) Å, respectively. The shortest distance between Ru^{II} Λ and Δ enantiomeric pair centres in **1** is 9.850(1) Å and it is of 8.676(7) Å in **2**, while the shortest distance between Ru^{II} same enantiomeric species (ΛΛ or ΔΔ) in **1** is 9.657(2) Å and it is of 8.760(5) Å in **2**.

The difference in geometries, excluding hydrogen atoms, between the two crystallographically independent complexes in **2**, was analysed by structural overlay analyses using Ru centres with N_1:N_2 phenanthroline ligands (r.m.s. deviation of 0.0037 Å) and Co centres with N7:C37:S1 isothiocyanate ligands (r.m.s. deviation of 0.0566 Å). The overlays presented in Figs. 8a and b indicate a difference between phenanthroline ligands and significant dissimilarities between isothiocyanate branches featured in minimum and maximum distances of 0.547 and 2.581 Å between the overlaid isothiocyanates sulphur atoms.

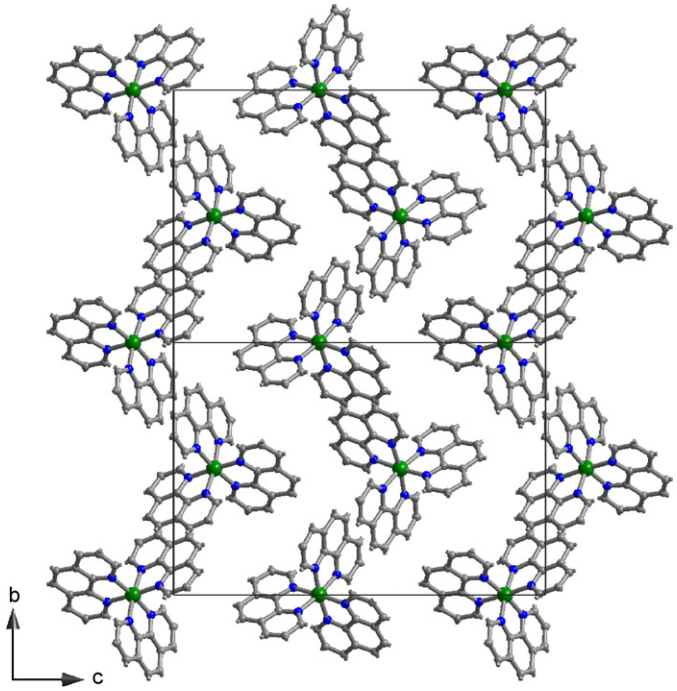

Fig. 5. A projection of $[Ru(phen)_3]^{2+}$ zigzag ΛΔΛΔΛ sequence of **1** in the *bc*-plane. $Fe(SCN)_4^{2-}$, SCN^- anions and water molecules were omitted for clarity.

In **2**, the crystal lattice is free of any geometrical constaints caused by solvates or counter ions interactions; hence, the packing pattern is entirely different from **1**. The $Co[(SCN)_4]^{2-}$ anions in **2** are oriented with a Co···Co shortest distance of 8.49(1) Å. The $Co[(SCN)_4]^{2-}$ anions are intruded in-between the $[Ru(phen)_3]^{2+}$ cations where, like in **1**, interacting together via C–H···S hydrogen bonds, at D···A average distance value of 3.58(1) Å. In particular, C22B–H22B···S4A (Table 3) is responsible for the intermolecular interactions in-between the double helices. However, a strong S···S intermolecular interaction is comprised in **2** between the inorganic modules at distance shorter than the revised compilation for the sum of van der Waal radii (4.06 Å) [20]. This interaction builds up a 1D helical chain through $Co(SCN)_4^{2-}$ inorganic anions. Such 'secondary-bonding' is probably a reason for the geometrical dissimilarities (Fig. 8) between $Co[(SCN)_4]^{2-}$ anions.

It has been noted [30] that in most of iso-thiocyanato metallates, although S···S intermolecular interaction is weak compared to other non-covalent forces like hydrogen bonds, it can act as a structural scaffold to associate the monomeric species into a polymeric extended structure. Recently, Ghosh et al. [31] had demonstrated the effective role of S···S interaction in the templating of $Hg(SCN)_4^{2-}$ with protonated 2,2′-dipyridylamine into 2D net.

The helical topology, formed by the S···S interaction in **2**, prompted us to make an analysis of the S···S interaction angles. The two S···S interactions in **2**, have for S1A···S2B interaction:

Table 3
Geometrical parameters of hydrogen bonds (Å, deg) involved between cationic–anionic species in **1** and **2**

	D–H···A	d(D–H)	d(H···A)	d(D···A)	DHA
1	O2–H41···O1	0.93(6)	1.75(6)	2.676(10)	176(7)
1	O2–H42···$S1^{i}$	0.85(6)	2.78(7)	3.465(8)	139(6)
1	O1–H39···$S3^{ii}$	0.89(5)	2.33(5)	3.215(8)	177(6)
1	O1–H40···N9	0.88(6)	2.09(5)	2.898(10)	154(6)
1	C3–H3···S1	0.95	2.91	3.79(1)	155
1	C21–H21···S3	0.95	2.92	3.70(9)	140
2	C1A–H1A···$S2A^{i}$	0.95	2.85	3.654(5)	143
2	C10A–H10A···$S4B^{ii}$	0.95	2.86	3.625(5)	139
2	C20A–H20A···$S1A^{iii}$	0.95	2.80	3.732(5)	167
2	C22B–H22B···$S4A^{iv}$	0.95	2.59	3.327(5)	134
1	C15–H15···$N9^{iii}$	0.95	2.50	3.36(1)	150
1	C22–H22···$N9^{iv}$	0.95	2.49	3.284(10)	141
1	C27–H27···$N9^{v}$	0.95	2.44	3.320(11)	155

For symmetry codes: **1** (i): 1/2−*x*, −1/2+*y*, 1/2−*z*, (ii): 1−*x*, 2−*y*, −*z*, (iii): 1/2−*x*, 1/2−*y*,−*z*, (iv): 1−*x*, 1−*y*, −*z*, (v): −1/2+*x*,−1/2+*y*, *z*. **2** (i): 1−*x*, 1−*y*, −*z*, (ii): 1/2−*x*, 1/2+*y*, 1/2−*z*, (iii): −1+*x*, *y*, *z*, (iv): 2−*x*, 1−*y*, −*z*.

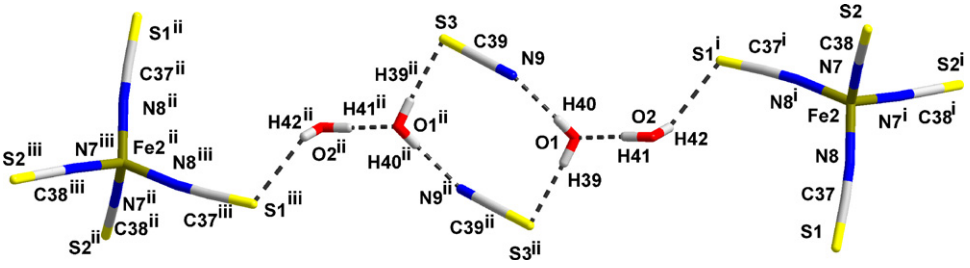

Fig. 6. Hydrogen bonding interaction modes in **1.** Symmetry codes: (i) 1/2−*x*, −1/2+*y*, 1/2−*z*, (ii) 1−*x*, 2−*y*, −*z*, (iii) 1/2−*x*,1/2−*y*,−*z*.

$\theta_1 = 117.51(2)^\circ$ and $\theta_2 = 153.61(2)^\circ$ (θ_1:C_1–$S_1\cdots S_2$, θ_2:$S_1\cdots S_2$–C_2) at distance of 3.966(2) Å and for S1B···S2A interaction: $\theta_1 = 93.60(2)^\circ$ and $\theta_2 = 161.99(2)^\circ$ at distance of 3.518(2) Å.

Recently, chalcogen–chalcogen interaction have been theoretically investigated and interpreted as nucleophilic–electrophilic interaction due to the anisotropic polarizability of sulphur atoms electron density [32]. We screened the CSD for isothiocyanate fragements showing S···S non-bonded interaction with distance range of 3.1–4.0 Å and found 461 non-disordered hits.

In Fig. 9, we show that roughly 3/4 of the structures fall close to the diagonal as $\theta_1 \approx \theta_2$. This represents an analogy to the symmetrical 'type-I' halogen–halogen interactions [13,33]. The two off diagonal clusters, with an abundance of almost 25 %, occur preferentially in the region of $\theta_{1,2}$: 140–180° and $\theta_{2,1}$: 60–110° and are thus representing the 'type-II' interaction.

As these two interaction types have been shown to be consistent with the calculated anisotropic electrostatic potential around bromine atoms in brominated organic compounds [13,33],

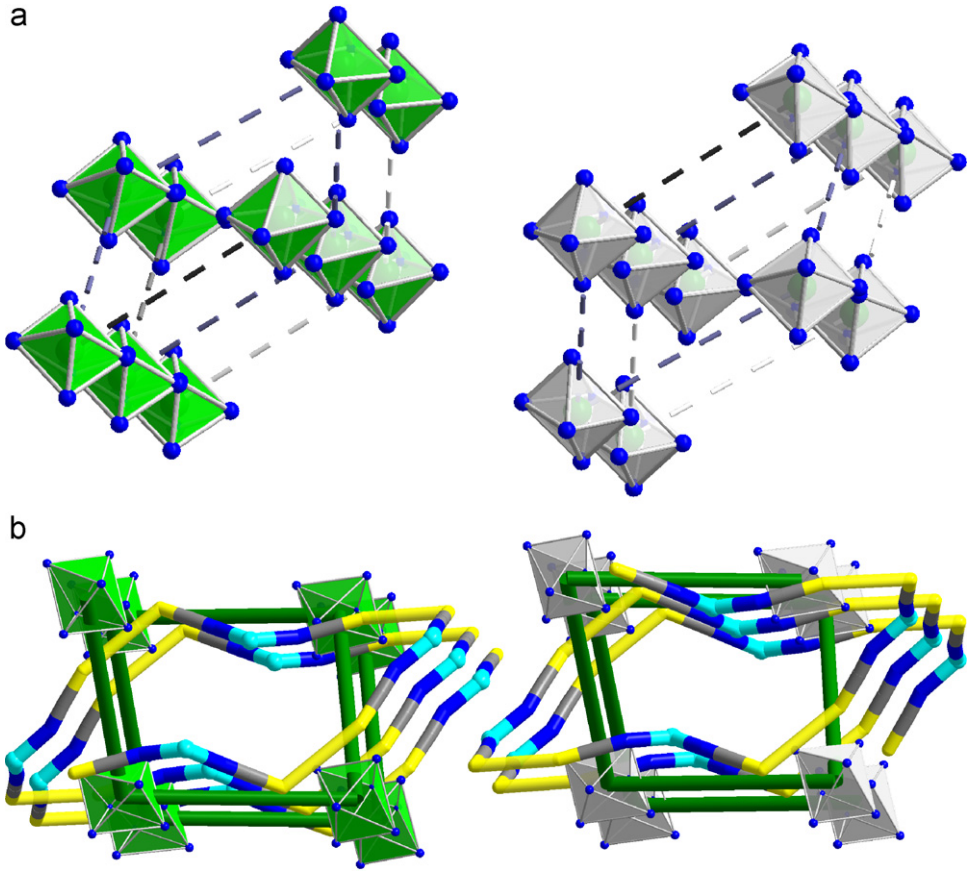

Fig. 7. (a) Perspective view of $[Ru(phen)_3]^{2+}$ Δ and Λ helices in **2**. (b) Homochiral 1D-double helices in **2**. In both (a) and (b), Λ- and Δ-$[Ru(phen)_3]^{2+}$ cations are presented as closed and open faces polyhedra, respectively. In (a), dotted lines show helical propagation in the *b*-direction. In (b) $Co(SCN)_4^{2-}$ helix caused by S···S interaction and $[Ru(phen)_3]^{2+}$ Δ- and Λ-helices are plotted.

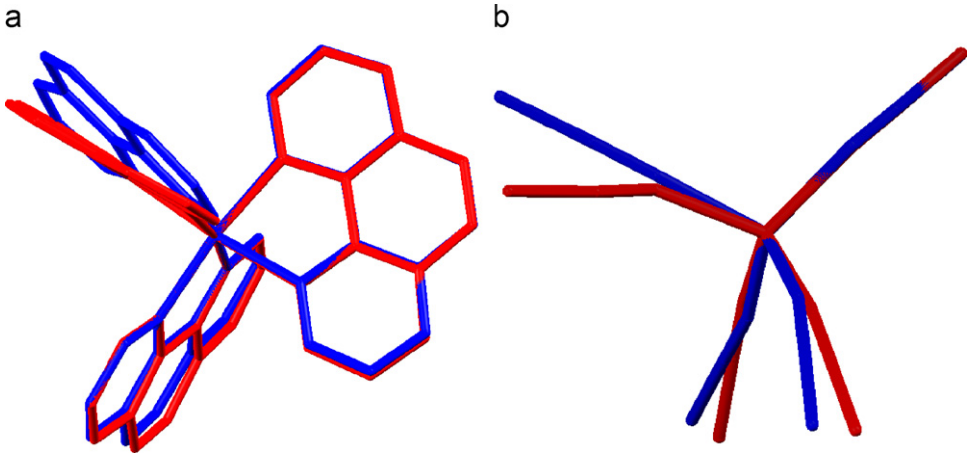

Fig. 8. Structural overlays of $[Ru(phen)_3]^{2+}$ (a) and $Co[(SCN)_4]^{2-}$ (b) in **2.**

we intended to see if a similar anisotropic electrostatic potential exists around the sulphur atoms in the isothiocyanate. In order to check this, a neutral model was needed as the electrostatic potential otherwise would be completely dominated by the overall negative charges of the complex ion.

Two models chosen to answer this relatively easy question are the neutral tetrahedral $\{Zn(NCS)_2(NCSH)_2\}$ and SCNH fragment, with a starting geometry taken directly from structure **1**. In the former, the Zn(II) ion is providing charge compensation, as well as a small perturbation of the electron density around sulphur, while avoiding unnecessary computational problems arising from different possible spin states of Fe(II) and Co(II). The resulting electrostatic potential is shown in Figs. 10a for SCNH and 10b for $\{Zn(NCS)_2(NCSH)_2\}$.

According to Fig. 10a, there is a central positive region and doughnut-like region of negative polarization, perpendicular to the C–S bond axis. In the case of tetrahedral $\{Zn(NCS)_2(NCSH)_2\}$, the negative electrostatic potential in Fig. 10b is extended over the space volume between the two sulphur atoms. It should be noted that this electrostatic model not only explains the two types of intermolecular bonds but also indicates that the type-II interaction should allow shorter intermolecular distances between the interacting centres. This is also what is found in **2** where the S···S pair closest in geometry to an ideal type-II interaction has the shortest S···S distance (3.518 Å vs. 3.966 Å).

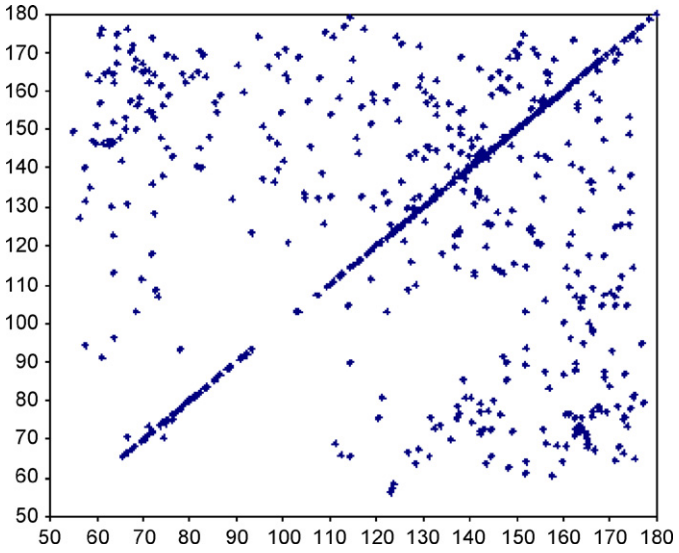

Fig. 9. The C–S_1···S_2–C angular distribution in 461 hits for interaction distance smaller than $2r_{vdW}$+0.4 Å.

In conclusion, we have synthesized two new mixed metal assemblies based on $[Ru(phen)_3]^{2+}$. We noted the role of hydrophobic forces and hydrogen bonds in the self assembly process of $[Ru(phen)_3]^{2+}$ with $Fe(SCN)_4^{2-}$. We have further shown that directional S···S interactions can have a significant role as a supramolecular 'synthons' with other stronger non-covalent interactions like hydrogen bonds and that they have similarities with the Br···Br intermolecular forces [13,33].

Supporting information and structures details

Crystallographic data for the structures reported in this paper have been deposited with the Cambridge Crystallographic Data Centre as supplementary publication no. CCDC 666224 and CCDC 666225. Copies of the data can be obtained free of charge on application to CCDC, 12 Union Road, Cambridge CB2 1EZ, UK (fax: +44 1223 336 033; e-mail: deposit@ccdc.cam.ac.uk).

Acknowledgment

Prof. Morsy Abu-Youssef, Alexandria University and Prof. Per Lincoln, Chalmers University of Technology are both gratefully acknowledged for their encouraging and valuable discussions. The financial aid from Chalmers University of Technology is acknowledged.

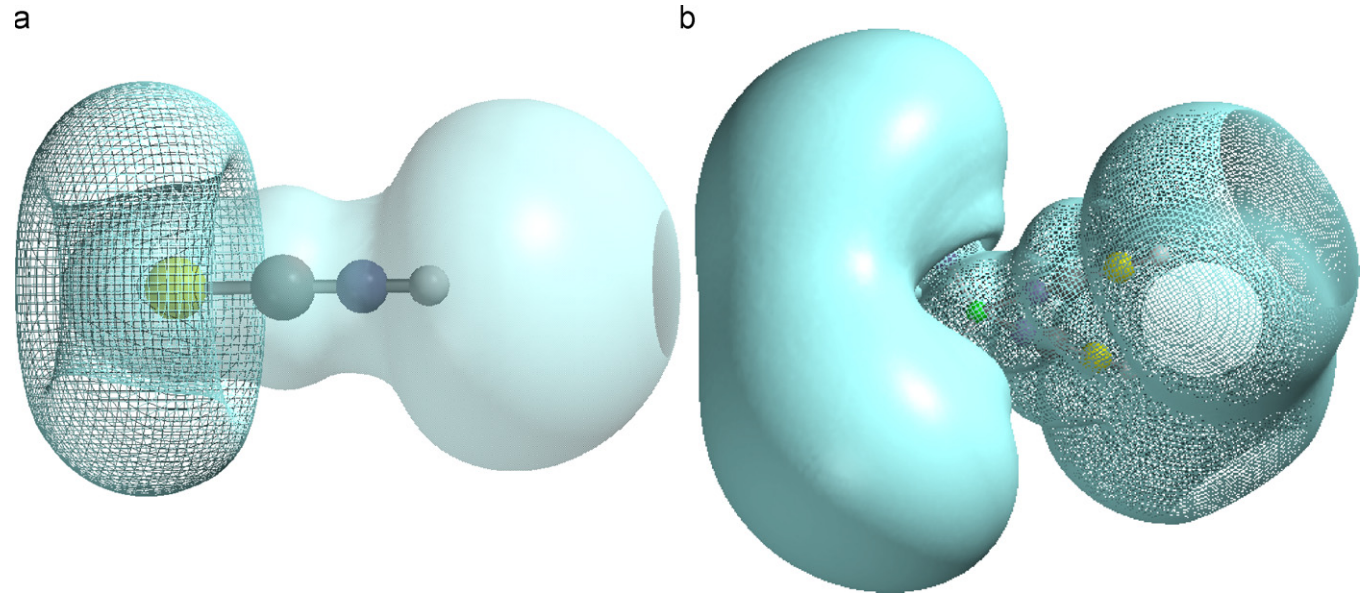

Fig. 10. Surfaces with isoelectrostatic potentials for SCNH (a) and $\{Zn(NCS)_2(NCSH)_2\}$, (b) calculated by DFT. In (a), −ve potential is presented in mesh and +ve potential in transparent surfaces. In (b), −ve potential is presented in solid and +ve potential in mesh surfaces. In both, positive +10 eV and negative −10 eV isoelectrostatic surfaces are plotted. The negative potential that surrounds the sulphur atoms has a doughnut-like surface leaving a space for some positive surface to "stick in" from the centre, in case of (a) resulting an anisotropic potential similar to that found for bromothiophenes, [13] consistent with the existence of type I and type II intermolecular interactions.

References

[1] J. Paharová, J. Černák, Z. Žák, J. Marek, J. Mol. Struct. 842 (2007) 117–124;
K. Adachi, Y. Sugiyama, K. Yoneda, K. Yamada, K. Nozaki, A. Fuyuhiro, S. Kawata, Chem. Eur. J. 11 (2005) 6616–6628;
T.-T. Luo, Y.-H. Liu, H.-L. Tsai, C.-C. Su, C.-H. Ueng, K.-L. Lu, Eur. J. Inorg. Chem. (2004) 4253–4258;
F. Setifi, S. Golhen, L. Ouahab, A. Miyazaki, K. Okabe, T. Enoki, T. Toita, J. Yamada, Inorg. Chem. 41 (2002) 3786–3790.

[2] E. Coronado, J.-R. Galán-Mascarós, C.-J. Gómez-García, J. Ensling, P. Gütlich, Chem. Eur. J. 6 (2000) 552–563.

[3] H.-J. Chen, L.-Z. Zhang, Z.-G. Cai, G. Yang, X.-M. Chen, J. Chem. Soc. Dalton Trans. (2000) 2463–2466.

[4] P. Vitoria, J. Beitia, J. Gutiérrez-Zorrilla, E. Sáiz, A. Luque, M. Insausti, J. Blanco, Inorg. Chem. 41 (2002) 4396–4404;
T. Steiner, Angew. Chem. Int. Ed. 41 (2002) 48–76;
O. Félix, M. Hosseini, A. De Cian, J. Fischer, Chem. Commun. (2000) 281–282.

[5] I.O. Fritsky, J. Swiątek-Kozlowska, A. Dobosz, T.Y. Sliva, N. Dudarenko, Inorg. Chim. Acta 357 (2004) 3746–3752;
A. Duda, A. Karaczyn, H. Kozlowski, I.O. Fritsky, T. Glowiak, E. Prisyazhnaya, T.Y. Sliva, J. Swiątek-Kozlowska, J. Chem. Soc. Dalton Trans. (1997) 3853–3860;
I.O. Fritsky, H. Kozlowski, E.V. Prisyazhnaya, Z. Rzaczynska, A. Karaczyn, T.Y. Sliva, T. Glowiak, J. Chem. Soc. Dalton Trans. (1998) 3629–3633.

[6] A. Clearfield, J. Wang, Y. Tian, E. Stein, C. Bhardwaj, J. Solid State Chem. 117 (1995) 275–289.

[7] I.O. Fritsky, J. Swiątek-Kozlowska, A. Kapshuk, H. Kozlowski, T.Y. Sliva, E. Gumienna-Kontecka, E.V. Prisyazhnaya, T. Iskenderov, Z. Naturforsch. B 55 (2000) 966–970.

[8] N. Zheng, H. Lu, X. Bu, P. Feng, J. Am. Chem. Soc. 128 (2006) 4528–4529.

[9] W. Dong, Y. Ou-Yang, H.-B. Song, D.-Z. Liao, Z.-H. Jiang, S.-P. Yan, P. Cheng, Inorg. Chem. 45 (2006) 1168–1172.

[10] C. Niezborala, F. Hache, J. Phys. Chem. A 111 (2007) 7732–7735;
N. Leventis, A.-M.M. Rawashdeh, I.A. Elder, J. Yang, A. Dass, C. Sotiriou-Leventis, Chem. Mater. 16 (2004) 1493–1506;
T. Urathamakul, J.L. Beck, M.M. Sheil, J.R. Aldrich-Wright, S.E. Ralph, Dalton Trans. 17 (2004) 2683–2690;
P. Lincoln, B. Nordén, J. Phys. Chem. B 102 (1998) 9583–9594.

[11] A. Galet, A.B. Gaspar, M.C. Muñoz, J.A. Real, Inorg. Chem. 45 (2006) 4413–4422;
A. Skorupa, B. Korybut-Daszkiewicz, J. Mroziński, Inorg. Chim. Acta 324 (2001) 286–292.

[12] A. Golub, H. Kohler, V. Skopenko, Chemistry of Pseudohalides, Elsevier, Amsterdam, 1986;
H. Zhang, X. Wang, K. Zhang, B.K. Teo, Coord. Chem. Rev. 183 (1999) 157–195.

[13] M. Ghazzali, V. Langer, C. Lopes, A. Eriksson, L. Öhrström, New J. Chem. 31 (2007) 1777–1784.

[14] SMART and SAINT: Area Detector Control and Integration Software, Bruker AXS, 2003, Madison, WI, USA.

[15] SADABS: Sheldrick G.M., Program for Empirical Absorption Correction of Area Detectors (Version 2.10), 2003, University of Göttingen, Germany.

[16] SHELXTL, Structure Determination Programs (Version 6.12), Bruker AXS Inc., Madison, WI, USA, 2001.

[17] DIAMOND: Program for Crystal and Molecular Structure Visualization (Version 3.1e), K. Brandenburg, Crystal Impact GbR, Bonn, Germany, 2007.

[18] F.H. Allen, Acta Crystallogr. B 58 (2002) 380–388.

[19] I. Dance, New J. Chem. 27 (2003) 22–27.

[20] S.C. Nyburg, C.H. Faerman, Acta Crystallogr. B 41 (1985) 274–279.

[21] Wavefunction, in 'SPARTAN '04, Ver. 1.0.3e', 18401 Von Karman Avenue, Suite Irvine, CA 92612, USA, 2006.

[22] B. Dalhus, C.H. Görbitz, Acta Crystallogr. B 56 (2000) 715–719.

[23] (a) J. Breu, A. Stoll, Acta Crystallogr. C 52 (1996) 1174–1177;
(b) J.-Z. Wu, Z.-Y. Zhou, L.-N. Ji, Cryst. Res. Technol. 36 (2001) 101–105.

[24] N. Motokawa, Y. Maeda, S. Hayami, Acta Crystallogr. E 63 (2007) m1521.

[25] A search in Cambridge Structure Database (CSD) [version 5.28, November 2006 with 3 updates] for Co(II)-tetra isothiocyanates has produced 42 non-disordered hits, from which 9 low-temperature measurements were analyzed. Minimum and maximum Co–N bond distances are 1.915–2.005 Å.

[26] L. Johansson, M. Molund, Å. Oskarsson, Inorg. Chim. Acta 31 (1978) 117–123.

[27] A.L. Spek, J. Appl. Crystallogr. 36 (2003) 7–13.

[28] D. Ben-Avraham, L.S. Schulman, S.H. Bossmann, C. Turro, N.J. Turro, J. Phys. Chem. B 102 (1998) 5088–5093.

[29] M.-L. Fu, G.-C. Guo, X. Liu, J.-P. Zou, G. Xu, J.-S. Huang, Cryst. Growth Des. 7 (2007) 2387–2389.

[30] H.-Y. Bie, J. Lu, J.-H. Yu, J.-Q. Xu, K. Zhao, X. Zhang, J. Solid State Chem. 178 (2005) 1445–1451.

[31] R. Ghosh, A.D. Jana, S. Pal, G. Mostafa, H.-K. Fun, B.K. Ghosh, Cryst. Eng. Commun. 9 (2007) 353–357.

[32] C. Bleiholder, D.B. Werz, H. Köppel, R. Gleiter, J. Am. Chem. Soc. 128 (2006) 2666–2674;
C. Bleiholder, R. Gleiter, D.B. Werz, H. Köppel, Inorg. Chem. 46 (2007) 2249–2260.

[33] F.F. Awwadi, R.D. Willett, K.A. Peterson, B. Twamley, Chem. Eur. J. 12 (2006) 8952–8960.